coatings

MDPI

Article

Effect of Cu, Zn and Ag Ion Implantation on the Surface Modification of Bacterial Cellulose Films

Izabela Betlej [1], Marek Barlak [2], Krzysztof Krajewski [1], Bogusław Andres [1], Zbigniew Werner [2], Agnieszka Jankowska [1,*], Sarani Zakaria [3] and Piotr Boruszewski [1,*]

[1] Institute of Wood Sciences and Furniture, Warsaw University of Life Sciences—SGGW, 159 Nowoursynowska St., 02-776 Warsaw, Poland
[2] Plasma/Ion Beam Technology Division, Material Physics Department, National Centre for Nuclear Research Świerk, 7 Sołtana St., 05-400 Otwock, Poland
[3] Materials Science Program, Department of Applied Physics, Faculty of Science and Technology, Universiti Kebangsaan Malaysia, Bangi 43600, Malaysia
* Correspondence: agnieszka_jankowska@sggw.edu.pl (A.J.); piotr_boruszewski@sggw.edu.pl (P.B.)

Abstract: The paper presents the preliminary results of cellulose modification by ion implantation. Three types of ions were implanted, i.e., copper, zinc and silver with fluences of 5×10^{14} and 5×10^{15} cm^{-2}, respectively. The acceleration voltage of the implanted ions was 30 kV. The ion penetration depth profiles showed differences, especially in the Cu and Ag cases, due to the different ion beams of these elements. The implantation of cellulose with ions clearly changed the wettability of the material surface in the direction of hydrophobicity. The impact of implantation on the growth of the cellulose surface by mold fungi was also noticeable. Only the silver ion implantation had a negative effect on the growth of the *Trichoderma viride* fungus but did not cause a complete inhibition of growth. Cellulose implantation with Cu and Zn ions clearly stimulated the growth of fungi on the surface of the polymer.

Keywords: bacterial cellulose; Ag; Cu; Zn ion implantation; surface modification; mold resistance; wettability

check for updates

Citation: Betlej, I.; Barlak, M.; Krajewski, K.; Andres, B.; Werner, Z.; Jankowska, A.; Zakaria, S.; Boruszewski, P. Effect of Cu, Zn and Ag Ion Implantation on the Surface Modification of Bacterial Cellulose Films. *Coatings* **2023**, *13*, 254. https://doi.org/10.3390/coatings13020254

Academic Editor: Carlo Antonini

Received: 30 December 2022
Revised: 17 January 2023
Accepted: 19 January 2023
Published: 21 January 2023

Copyright: © 2023 by the authors. Licensee MDPI, Basel, Switzerland. This article is an open access article distributed under the terms and conditions of the Creative Commons Attribution (CC BY) license (https://creativecommons.org/licenses/by/4.0/).

1. Introduction

Cellulose is one of the most commonly used polymers that are available abundantly. Due to its very good mechanical properties and non-toxicity, it can be used for numerous applications, e.g., as a packaging material, construction material, textile material and a medical device as a dressing material [1–4]. Cellulose derivatives, especially cellulose ethers, are widely used in cosmetology and pharmaceutical production [5]. Obtaining cellulose from plant tissue is not different to the obtained quality of the cellulose itself. Obtaining cellulose from wood is associated with its partial depolymerization, but also with the introduction of harmful substances into the environment, such as sulfur, nitrogen or chlorine compounds. Moreover, the process of obtaining cellulose from plant biomass requires large amounts of energy and water consumption [6]. An alternative source of obtaining cellulose may be through microorganisms synthesizing. Numerous studies have indicated that microorganisms, especially bacteria belonging to *Komogataeibacter*, can produce a cellulose polymer with a relatively high degree of polymerization and high crystallinity, which successfully substitutes plant cellulose [7–9]. Very favorable physical and mechanical properties of bacterial cellulose make it a potentially promising polymer with a wide range of applications. Undoubtedly, the unusual ease of modifying the structure of this type of polymer means that it can obtain unprecedented features, enabling the expansion and diversification of the areas of its application [10]. In addition, bacterial cellulose is an environmentally attractive material because it is biodegradable, nontoxic

and can be obtained at relatively low costs using microbiological substrates based on waste plant materials from agriculture or the food industry [11,12].

Cellulose modification is a process aimed at improving the properties of cellulose. Modification can be carried out at the synthesis stage, in situ, by introducing substances into the microbial medium that are incorporated directly into the polymer structure [13], or in vitro, after the production of the polymer [14]. Polymer modification methods lead directly to changes in the polymer, giving the material new physical, mechanical or chemical properties dedicated to specific applications. The modification of cellulose can lead to changes in its surface roughness, adhesion, wettability and surface free energy, and it can also lead to the acquisition of new chemical and biological properties, such as chemical reactivity as well as antibacterial properties [15–18].

Examples of cellulose modification with electron or ion beams have been reported by many researchers. For example, electron beam irradiation of lignocellulosic material showed that changes in the wettability of lignocellulosic materials depend on the number and energy density of electron pulses [19].

In the case of ion implantation, depending on the type of ions, their dose, energy and beam current density, a series of physical and chemical reactions can be induced in materials, leading to completely new properties [20]. Leveneur et al. [21] showed that the ion beam implantation of polymers generates mainly radical, cross-linking and bond breaking reactions. The same authors, subjecting the cellulose material to implantation with low-energy N, O and Ar ions, showed significant structural and chemical changes in the tested material. In another study by Shanthini et al. [22], implantation of a cellulose-based composite with a beam of N^{3+} ions with an energy of 24 keV in fluences of 1×10^{15}, 5×10^{15} and 1×10^{16} ions/cm^2 increased the roughness and modified the luminescent and thermal properties of the tested composite. Changes in the cellulose microstructure due to the breaking of intramolecular and intermolecular hydrogen bonds were demonstrated by Zhang et al. [23] by subjecting cellulose to implantation with low-energy N^+ ions. Implantation of bacterial cellulose with He^+ and Ar^+ ions with fluences of 1×10^{15} and 1×10^{16} cm^{-2}, with an ion energy of 60 keV, increased the hydrophobicity of the polymer surface [24]. The increase in hydrophobicity is attributed to the degradation of the polar groups during the implantation process [25].

Changes in the polymers' structure during the implantation process can be controlled by appropriate selection of the type and dose of implanted ions, their energy and ion current density. Low doses of ions lead to porosity of the material, while higher doses facilitate the formation of cross-linked structures [15]. It has been shown that helium ions penetrate deeper into bacterial cellulose than argon ions [24]. It has also been proven that large ions remain more easily in the polymer substrate than small ions that are released along with gaseous by-products of the implantation process [26].

This paper presents the preliminary results on changes in wettability and susceptibility to mold growth of the surface of bacterial cellulose implanted with the ions of transition metals such as Cu, Zn and Ag. The implanted elements were selected based on their use in other cellulose and wood protection treatments currently in practice. Ion implantation processes were preceded by simulation tests using the Monte Carlo method of the main parameters of the depth profiles of the implanted elements, allowing us to determine the depth of penetration and distribution of the implanted ions in the polymer.

2. Materials and Methods

2.1. Cellulose and Its Preliminary Investigations

Bacterial cellulose (BC) was obtained in the process of culturing microorganisms called SCOBY (Symbiotic Culture of Bacteria and Yeast) on a medium containing 10% food sucrose (Krajowa Spółka Cukrowa SA, Toruń, Poland) and 0.03% peptone (Biomaxima SA, Lublin, Poland). The method of cultivation leading to the acquisition of cellulose and the method of its purification were carried out in accordance with the procedure described in a previous publication [27]. The purified cellulose was dried in a laboratory dryer

(J.P. Selecta Laboratory Equipment Manufacturer, Barcelona, Spain), at a temperature of 24 ± 2 °C, until a constant polymer weight was obtained. Cellulose sheets with dimensions of 200 × 500 mm^2 and a thickness of 0.13 ± 0.02 mm were used for the ion implantation.

2.2. Modlling and Ion Implantation

Cu with the atomic mass of 63.546 u and the atomic radius of 128 pm, Zn with the atomic mass of 65.38 u and the atomic radius of 139 pm and Ag with the atomic mass of 107.8683 u and the atomic radius of 172 pm were selected as the elements to the modification of cellulose using ion implantation method.

The ion implantation processes were preceded by Monte Carlo simulations (modeling) of the main parameters of the depth profiles of the implanted elements (such as the peak volume dopant concentration N_{max}, projected range R_p, range straggling ΔR_p, kurtosis and skewness) [28] using freeware-type code SRIM-2013.00 (The Stopping and Range of Ions in Matter). The simulation was performed for 100,000 implanted ions of Cu, Zn and Ag, perpendicular to the implanted target (the angle of the ion incidence was defined as 0°). The theoretical values of the sputtering yield Y were additionally calculated using the commonly known freeware-type quick ion implantation calculator SUSPRE, and theoretical values from the energy deposited in the surface region of the material were calculated using the Sigmund formula.

The modeled substrate material C-H-O (modeling codes treat the sample as a set of atoms that do not form chemical compounds) had a composition of 44.5% carbon, 6.2% hydrogen and 49.3% oxygen in atomic percentages. The substrate material density adopted for the simulation was 1.583 g/cm^3. All above values were determined for the real material, as mentioned above.

In all cases, the modeling/calculations were performed for room temperature. The fluences of the implanted ions were 5 × 10^{14} and 5 × 10^{15} cm^{-2}. The value of the acceleration voltage was taken at 30 keV. Due to the ion implantation without mass separation, the ion beam contained several kinds of ions with different degrees of ionization. In addition, the percentage shares of individual ion types are were different (Table 1). The use of all data for the selected element is usually cumbersome; therefore, the average charge state (ACS) is a more popular parameter for the modeling as an equivalent of the sum of profiles for the individual ion kinds. The average charge state is determined by adding the values of multiplication of the percentage shares and the ionization's degree. For example, for Cu, it will be:

$$0.28 \times 1 + 0.53 \times 2 + 0.18 \times 3 + 0.01 \times 4 = 1.92 \approx 1.9 \quad (1)$$

Table 1. The percentage charge state distribution and average charge state of several elements [29].

Implanted Ions	Ion energy for Acceleration Voltage of 30 kV				Average Charge State/ACS Ion Energy (keV)
	30 keV	60 keV	90 keV	120 keV	
	Percentage Charge State Distribution (%)				
	1+	2+	3+	4+	
$Cu^+ + Cu^{2+} + Cu^{3+} + Cu^{4+}$	28	53	18	1	1.9/57
$Zn^+ + Zn^{2+}$	80	20	-	-	1.2/36
$Ag^+ + Ag^{2+} + Ag^{3+} + Ag^{4+}$	13	61	25	1	1.9/57

Therefore, the ACS Cu ion energy is 57 keV for the acceleration voltage of 30 kV (1.9 × 30 = 57).

The modeling did not account for the phenomenon of substrate sputtering by the implanted ions, substrate damages and the chemical reactions between the implanted ions and/or the substrate components.

The ion implantation processes were performed using a MEVVA (Metal Vapor Vacuum Arc) type implanter, with non-mass separated pulse beam based on Brown and Washburn [30].

The fluence of implanted ions was the same in all cases, and it was 5×10^{14} and 5×10^{15} cm^{-2}. The value of the acceleration voltage was 30 kV. The beam current was at a level of 100 mA for the cross-sectional area of the ion beam of about 80 cm^2. The beam current density was at a level of about 1.25 mA/cm^2.

The implanted cellulose samples in the sample holder (Figure 1) were clamped onto a stainless-steel plate to avoid overheating effects, so the estimated value of temperature of the implanted pieces and the measured value of the sample holder did not exceed 50 °C. The working pressure in the vacuum chamber was at a level from 2 to 5×10^{-3} Pa.

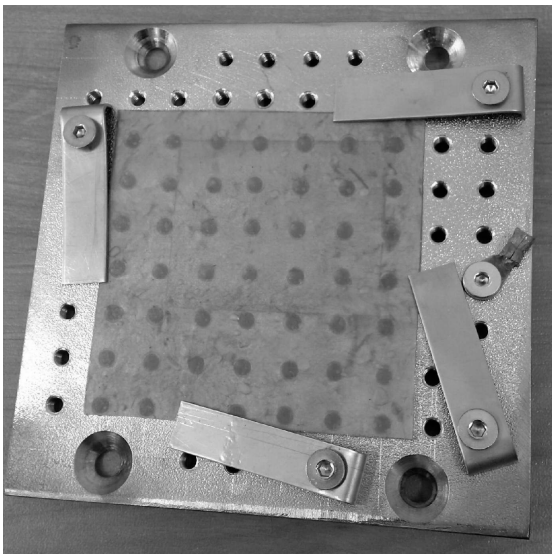


Figure 1. The implanted cellulose in the steel sample holder.

2.3. Determination of the Contact Angle

The surface contact angle of the virgin and modified cellulose was determined using a Haas Phoenix 300 goniometer (Surface Electro Optics, Suwon City, Korea). An image analysis system (Image XP, Surface Electro Optics, version 5.8, Suwon City, Korea) was used to determine the angle between the tangent to the drop contour and the straight line crossing its base. The analysis of the change in wettability was carried out after 5, 20, 40 and 60 s from the moment of water droplet deposition on the sample surface. Measurements were performed in air with a humidity of 50% and a temperature of 21 ± 2 °C according to the methodological guidelines presented by Wolkenhauer et al. [31]. Measurements were performed in 10 replications.

2.4. Resistance to Molds

Discs with a diameter of 20 mm were cut out of bacterial cellulose, which was then sterilized in UV light (Bionovo, Legnica, Poland). Sterile discs were placed on a maltose medium containing 2.5% maltose extract (Linegal Chemicals sp. zo.o., Blizne Łaszczyńskiego, Poland) and 2.5% agar (Polaura, Morąg, Poland). Plastic, sterile pads separated the cellulose from direct contact with the moist substrate. The inoculum of mold fungi was placed at four equal distances around the discs. Each inoculum was placed approximately 10 mm from the edge of the cellulose samples. Two species of fungi from the pure cultures collection of the Institute of Wood Sciences and Furniture of the Warsaw University of Life Sciences were used for inoculation: *Trichoderma viride* Pers., strain A-102 and *Chaetomium globosum* Kunze, strain A-141 (ATCC 6205). The fungi were grown in a Thermolyne Type 42,000 thermal incubator (ThermoFisher Scientific, Waltham, MA, USA) for 8 days at 26 °C. Mold growth was documented daily by taking high-resolution images

on a laboratory photo-taking station. The assessment of the degree of fungal fouling on the surface of the samples was determined based on the guidelines of the methodology described by Borysiuk et al. [32]. The percentage of fungus coverage of the cellulose surface was calculated relative to the total cellulose surface. The percentage of cellulose surface fouling was determined with an accuracy of 5% using ImageJ2 image analysis software (Fiji v1.52i). The test was performed in three repetitions for each cellulose variant and for each species of fungus.

2.5. SEM Analysis

The observations of the virgin, ion implanted and mold tested on cellulose surface were performed using Scanning Electron Microscopy. The observations were performed for an acceleration voltage of 20 kV and for the magnification of, e.g., 500, 1000 and 2000×. Two detectors, i.e., a secondary electron detector (marked as SE or SED) and backscattered electron detector (BSE or BSD), were used for the observations. The samples were covered by a 5 nm gold layer before the observations.

2.6. Test Standards

The analysis of variance (ANOVA) was used to investigate significant differences between the variants of the tested materials. The comparison of means was performed with the Tukey test. In general, the mean values of the studied parameters were compared with one-way analysis of variance (ANOVA) and the post-hoc Tukey test, in which homogeneous groups of mean values for each parameter were identified for $p = 0.05$. Statistical analysis of the results was performed using Statistica version 13 (TIBCO Software Inc., Palo Alto, CA, USA).

3. Results and Discussion

The obtained results (excluding the modeling results) are presented for higher fluence (5×10^{15} cm^{-2}) of the implanted ions. Only with this fluence a positive effect on changes in the degree of fouling of the cellulose surface by mold fungi was observed.

3.1. Modeling of the Cu, Zn and Ag Ion Implantation

Figure 2 and Table 2 present the results of the computer simulations of the depth profiles of ions implanted without t*he* mass separation to C-H-O material. The results obtained for Cu, Zn and Ag ions implantation were presented at the same scales for better comparison.

The presented "SRIM units" in (atoms/cm^3)/(atoms/cm^2) are a special units of plot ordinate used in SRIM code results. With these units, by multiplying by the ion fluence (in atoms/cm^2), the ordinate values convert directly into a density distribution with the unit of atoms/cm^3. The results of such calculations are presented in Table 2 for both used fluencies of the implanted ions.

The values presented without the brackets were obtained for real cases of the ion implantations, while the values presented in the brackets are the values for ACS case calculations.

The modeled partial (thin solid lines) and summary (bold solid lines) real and ACS (dotted lines) depth profiles, presented in Figure 2 (left), are different, especially in the Cu and Ag cases, due to the differentiated ion beams of these elements. In the Cu ion implantation case, the real profile is very different from the classical Gaussian distribution, and the ACS equivalent should not be used in these considerations. This is also confirmed by the significant differences in the values presented in Table 2, especially for the SRIM units and therefore for the peak volume dopant concentration, range straggling, skewness and kurtosis. It is slightly better in the case of Ag ion implantation. The maximum SRIM units' values were similar for the real and ACS cases; however, the difference in the skewness was about 50%. The smallest differences were observed for the modeling of Zn ion implantation and were related to the presence of only two types of ions in the beam,

which had shares of 80 and 20%. In this case, the use of ACS is fully legitimate and can simplify modeling processes.

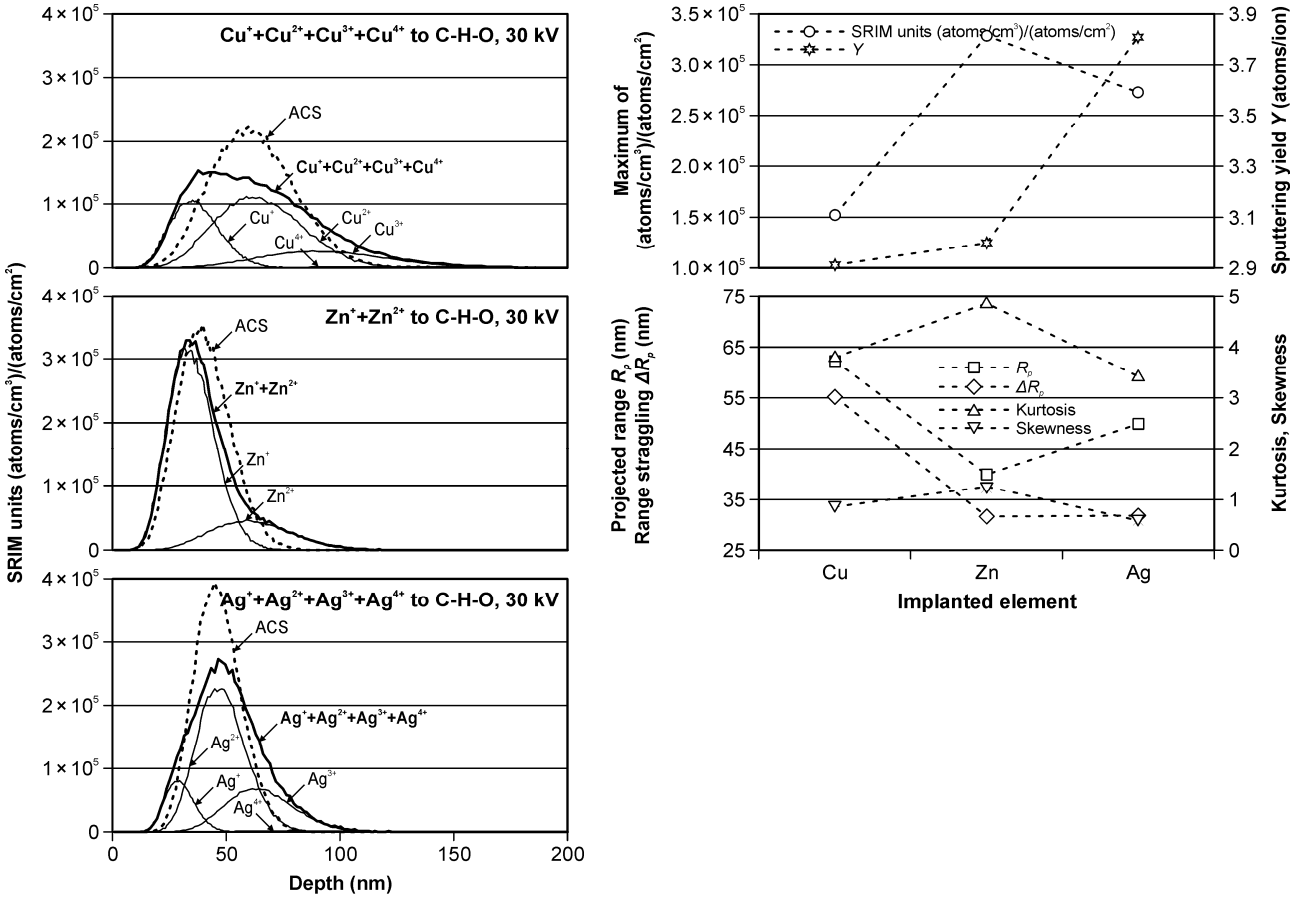


Figure 2. The modeled Cu, Zn and Ag ions depth profiles in C-H-O material (**left**); The modeled values of SRIM units, sputtering yield, projected range, range straggling, kurtosis and skewness as functions of the implanted elements (**right**).

Table 2. The peak parameters and sputtering yield values for all implanted cases.

Implanted Ions	$Cu^+ + Cu^{2+} + Cu^{3+} + Cu^{4+}$	$Zn^+ + Zn^{2+}$	$Ag^+ + Ag^{2+} + Ag^{3+} + Ag^{4+}$
Maximum SRIM units (atoms/cm^3)/(atoms/cm^2)	1.52×10^5 (2.23×10^5)	3.29×10^5 (3.55×10^5)	2.73×10^5 3.95×10^5
Peak volume dopant concentration N_{max} (cm^{-3}) for fluence of 5×10^{14} cm^{-2}	7.6×10^{19} (1.11×10^{20})	1.65×10^{20} (1.77×10^{20})	1.37×10^{20} (1.98×10^{20})
Peak volume dopant concentration N_{max} (cm^{-3}) for fluence of 5×10^{15} cm^{-2}	7.6×10^{20} (1.11×10^{21})	1.65×10^{21} (1.77×10^{21})	1.37×10^{21} (1.98×10^{21})
Projected range R_p (nm)	62.3 (61.7)	40 (40)	49.9 (46)
Range straggling ΔR_p (nm)	55.2 (36)	31.6 (22.8)	31.8 (20.4)
$R_p/\Delta R_p$ ratio	1.13 (1.71)	1.27 (1.75)	1.57 (2.25)
Skewness	0.85 (0.34)	1.23 (0.35)	0.58 (0.32)
Kurtosis	3.83 (2.99)	4.89 (2.98)	3.44 (3.04)
Sputtering yield Y (atoms/ion)	2.91 (2.99)	3 (3.05)	3.81 (4.37)

Figure 2 (right) shows the modeled values of SRIM units, sputtering yield, projected range, range straggling, skewness and kurtosis for the real depth profiles as a function of the implanted elements.

SRIM units' value was the highest for Zn ion implantation, which, in combination with a relatively low sputtering value, made it possible to obtain a relatively high concentration of this element in the peak. It was different than the other cases. The maximum SRIM units' value was relatively high for Ag ion implantation, but the sputtering was highest in the comparison in the Zn ion case. Contrary, the sputtering was smallest for Cu ion, but the maximum SRIM units' value was also the smallest.

The projected range indicates that the location of the center of the peak was highest for Cu and smallest for the Zn ion, and the range straggling, being an indicator of the peak width, was also highest for Cu ion and smallest and very similar for the Zn ion and Ag ion. The skewness and kurtosis, indicating a deviation from the classical Gaussian curve, changed in the range from 0.58 to 1.23 and from 3.44 to 4.89, respectively.

3.2. Wettability of Bacterial Cellulose after Ion Implantation

The results of the contact angle change in the time of 5, 20, 40 and 60 s during the water wettability tests of the virgin and all implanted samples are presented in Figure 3. In addition, the numerical values of the contact angle and the bars of standard deviations are marked. Figure 4 presents the percentage contact angle change relative to start point of the measurements, i.e., 5 s (left) and relative to virgin values (right), in the time.

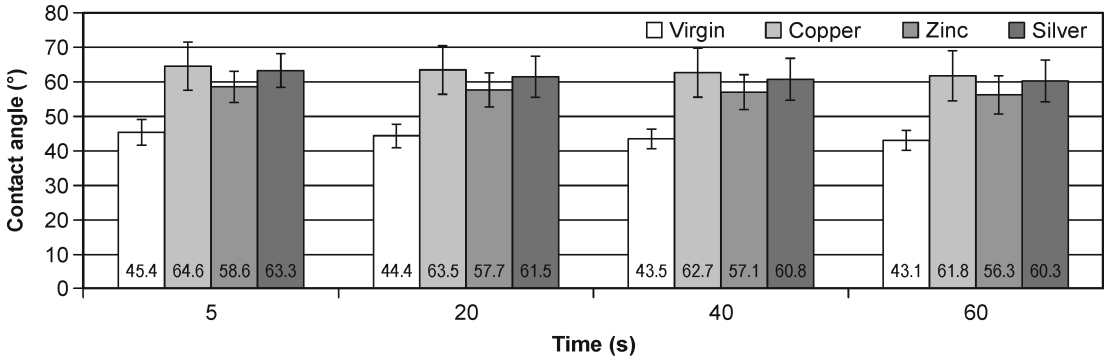


Figure 3. The change of the contact angle in the time for virgin and implanted cellulose.

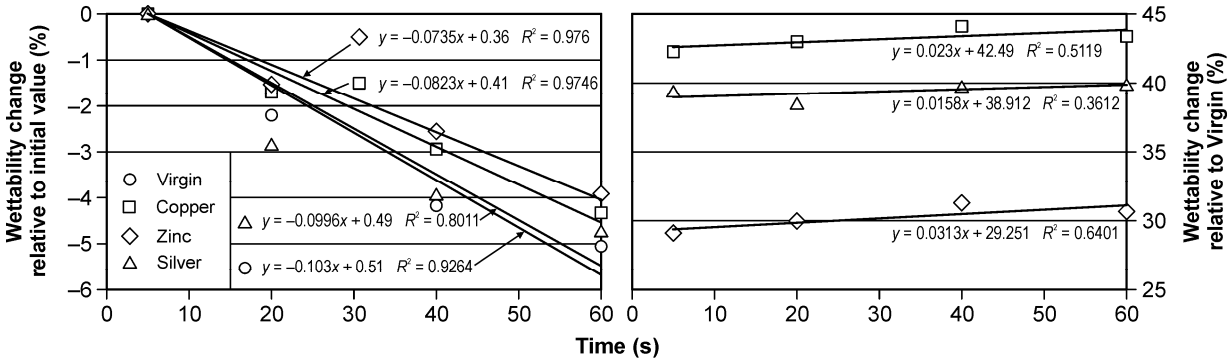


Figure 4. The percentage change of the contact angle in the time for virgin and implanted cellulose: relative to initial value (**left**) and relative to virgin samples value (**right**).

It should be noted that the ion implantation of all elements increases the hydrophobic of cellulose, the most for Cu ion, the least for Zn ion. The percentage change for Cu implantation is about 44% and for Zn implantation is about 30%. The time change within the same modifications is less than 6%. It is very similar result for all types of the investigated samples.

Measurements of the contact angle confirmed that the implantation process caused significant changes in the wettability of the cellulose surface. The surface of the modified cellulose became less hydrophilic than the original polymer (Figure 3). There were no significant differences in surface wettability between the variants of modified cellulose (Table 3). Implantation with Cu, Zn and Ag ions using ion beam therefore produced similar changes in the surface wettability. The results of the contact angle measurements showed slight changes in the wettability after 60 s from the deposition of a drop of water on the treated cellulose. Minor changes were also observed in the native cellulose. The implantation of the metal disturbed the hydroxyl group and the inter and intra H bonding that make them less hydrophilic [15].

Table 3. Statistical evaluation (ANOVA) of the ions influencing wettability of the bacterial cellulose surface.

Factor	Sum of Squares	Mean Sum of Squares	Fisher's F-Test	Significance Level
	SS	**MS**	**F**	***p***
Intercept	134,589.0	134,589.0	4623.433	0.000000
Modifier	2305.4	768.5	26.399	0.000000
Error	1048.0	29.1		

Figure 4 shows time-dependent changes in the relative value of changes in the cellulose contact angle. It should be noted that for each type of implantation, these changes are close to linear (for the graph on the left), and a slight increase in wettability was observed for each of the tested surfaces. The difference in the contact angle between the implanted surfaces ranged from less than 5 (between the surface implanted with silver and copper) to 15% (between the surface implanted with zinc and copper). The relative change of the contact angle was very similar for all tested cases; however, it was smallest for ionic silver implantation. Negative values indicate that the contact angle decreased.

In addition, in the studies of their other authors, it can be seen that the process of ion implantation led to changes in the wettability of the surface [33]. Suzuki et al. [34] showed that changes in the wettability of implanted materials depend on the type of ions and fluences, while Barlak et al. [19] found that changes in the surface properties of implanted materials depend on the number and energy density of electron pulses.

3.3. Mold Growth on Bacterial Cellulose Surface

The analysis results of the influence of bacterial cellulose modification on the activity of microorganisms on its surface are presented in Table 4. By assessing the degree of growth of mold fungi on the surface of ion beam-modified cellulose, it was found that the presence of the changed surface stimulated the growth of the fungus *Ch. globosum* for its growth (Table 5). Particularly intensive growth of the fungus was observed on the surface implanted with zinc ions. In addition, the growth rate of *Ch. globosum* on the surface implanted with copper ions was much larger than on the control cellulose surface. The weakest growth was observed on the surface of cellulose implanted with silver ions. The growth of *T. viride* fungus on the cellulose surface was less dynamic, but the growth of the fungus was clearly inhibited on the cellulose surface implanted with a beam of silver ions. This observation was not confirmed by ANOVA (Table 6); however, based on the post-hoc Tukey test (Table 4), Ag^+ ion modification was the most effective in preventing fungus growth.

Table 4. Percentage growth of mold on the surface of bacterial cellulose depending on the implantation with a beam of Cu, Zn and Ag ions.

Microorganism	Type of Ion Implantation	Growth of Mold on Bacterial Cellulose (%)				
		1 day	2 day	3 day	4 day	5 day
Trichoderma viride	Virgin	0	0	0	25.07 ab	37.54 ab
	Ag	0	0	0	9.17 a	22.83 a
	Cu	0	0	0	19.00 ab	38.95 ab
	Zn	0	0	0	34.26 b	51.45 b
Chaetomium globosum	Virgin	0	0	0	34.26 b	51.45 a
	Ag	0	32.23 a	48.69 a	56.52 a	60.33 a
	Cu	0	40.28 a	53.29 a	59.71 a	65.65 a
	Zn	0	53.62 ab	68.89 ab	71.75 ab	76.89 ab

a, ab, b—the homogeneous groups by the Tukey test.

Table 5. Statistical evaluation (ANOVA) of the influence kind of implementation on the growth of *Chaetomium globosum* on the bacterial cellulose surface.

Factor	Sum of Squares	Mean Sum of Squares	Fisher's F-Test	Significance Level
	SS	MS	F	*p*
Intercept	69,760.25	69,760.25	901.5027	0.000000
Modifier	1627.02	542.34	7.0086	0.008049
Error	773.82	77.38		

Table 6. Statistical evaluation (ANOVA) of the influence kind of implementation on the growth of *Trichoderma viride* on the bacterial cellulose surface.

Factor	Sum of Squares	Mean Sum of Squares	Fisher's F-Test	Significance Level
	SS	MS	F	*p*
Intercept	20,981.08	20,981.08	92.62361	0.000001
Modifier	1410.90	470.30	2.07620	0.161598
Error	2491.72	226.52		

3.4. SEM Analysis

Figure 5, for example, shows the differences in the defects in Cu, Zn and Ag ions implanted cellulose treated with *T. viride* fungus. In this case, the influence of the fungal hyphae on the changes occurring on the polymer surface is clearly visible. Clear cracks observed in the cellulose implanted with zinc ions indicate that the metal ion present on the surface does not have a fungal growth-inhibiting effect, which correlates with high fungal growth activity. The cellulose surface implanted with silver ions did not show damage in the form of cracks despite of the observed slight growth near the edge of the sample. It can therefore be concluded that the biocidal efficacy of silver ions against *T. viride* has been confirmed.

The presented experiment showed that the low-energy implantation of zinc, copper and silver ions influenced changes in the wettability of the cellulose surface and its susceptibility to mold growth. At this stage of research, the reasons for the occurrence of the phenomena have not been verified, but it can be assumed that both the energy and the dose of implantation contribute to changes in intra- and intermolecular interactions [23]. As suggested by the same authors, the implantation process implies the formation of structural changes in cellulose. SEM analysis of the cellulose-based composite implanted with N^{3+} ions with an energy of 24 keV at fluences of 1×10^{15}, 5×10^{15} and 1×10^{16} cm^{-2} revealed the formation of microstructures that led to changes in the thermal and mechanical

properties of the tested material [22]. Parakrajank et al. [35] found that chitosan–cellulose membranes changed the surface roughness of the membrane, as well as the wettability, impedance, conductivity and capacity, when bombarded with beams of argon and nitrogen ions with an energy of 15–25 keV. It was also found that changes in wettability depend on the type of material and the ionic fluence number. In the presented research results, it can be concluded that the implantation process itself has an impact on wettability and, to a lesser extent, the type of ions used.

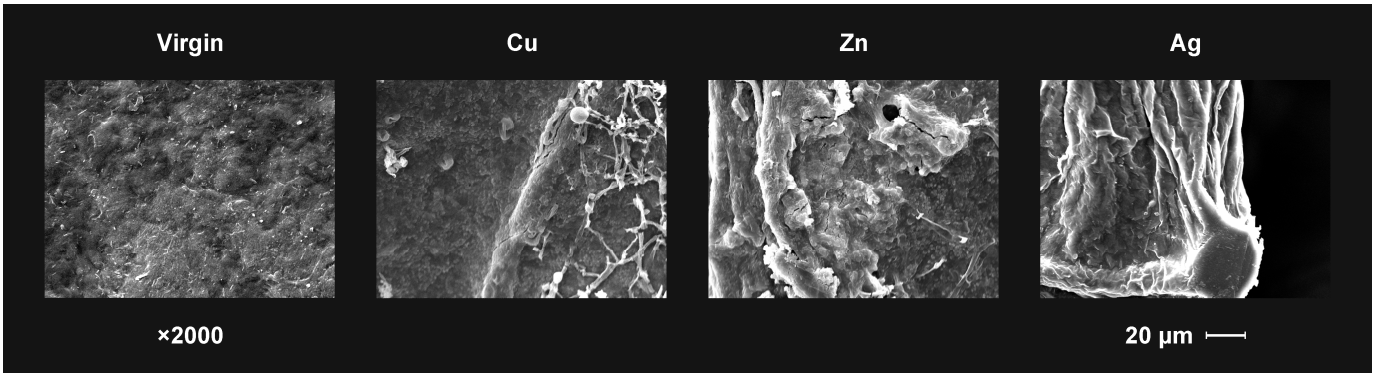


Figure 5. The SEM observation results of the virgin and the ion implanted bacterial cellulose surface after *T. viride* growth at day 5 in the test.

The effect of ion implantation on changes in the material properties was also confirmed for other polymers and materials [36,37]. Nowak et al. [38] showed that the implantation of a sapphire crystal with Ag ions caused damage to the crystal lattice, which resulted in a decrease in the value of Young's modulus. Crystal lattice damage may be related to the depth profile of the ions in the material, which, in turn, is related to the value of the fluence used or the sputtering efficiency [24]. The presented studies confirmed the differences in the depth of ion penetration into the structure of the material in the process of ion implantation. Determining whether these differences affect the obtained changes in the degree of cellulose fouling by fungi, wettability and other physical and mechanical characteristics not presented in this publication will be the subject of further work by the authors.

4. Conclusions

The presented results showed changes in wettability and the degree of fouling by fungi on the surface of bacterial cellulose subjected to implantation with zinc, copper and silver ions. The ions used affected changes in the observed properties of the polymer. It should be noted that the hydrophobicity of the implanted cellulose increased in all cases. It can therefore be concluded that the applied method of chemical modification of bacterial cellulose is also a good tool for the physical modification of the polymer surface. Modeling the profile of the depth and range of penetration of the implanted ions into the material structure showed that the value of SRIM units was the highest for Zn implantation, while the impact of the depth of ion penetration in the implantation process and changes in the molecular structure of bacterial cellulose require in-depth research and further analyses.

Author Contributions: Conceptualization, I.B. and M.B.; methodology, I.B., M.B., K.K., P.B., B.A. and Z.W.; software, I.B., A.J. and M.B.; validation, I.B. and P.B.; formal analysis, I.B.; investigation, I.B. and P.B.; resources, I.B.; data curation, I.B., M.B. and P.B.; writing—original draft preparation, I.B. and M.B.; writing—review and editing, P.B. and S.Z.; visualization, I.B.; supervision, I.B.; project administration, I.B. and A.J. All authors have read and agreed to the published version of the manuscript.

Funding: This research received no external funding.

Institutional Review Board Statement: Not applicable.

Informed Consent Statement: Not applicable.

Data Availability Statement: Not applicable.

Acknowledgments: The authors thank the Warsaw University of Life Sciences (SGGW) for financial support. Many thanks to Jerzy Zagórski and Bogdan Staszkiewicz for technical assistance.

Conflicts of Interest: The authors declare no conflict of interest.

References

1. Sirviö, J.A.; Liimatainen, H.; Niinimäki, J.; Hormi, O. Sustainable packaging materials based on wood cellulose. *RSC Adv.* **2013**, *37*, 16590–16596. [CrossRef]
2. Nasir, M.; Aziz, M.A.; Zubair, M.; Manzar, M.S.; Ashraf, N.; Mu'azu, N.D.; Al-Harthi, M.A. Recent review on synthesis, evaluation, and SWOT analysis of nanostructured cellulose in construction applications. *J. Build. Eng.* **2022**, *41*, 103747. [CrossRef]
3. Šauperl, O.; Stana-Kleinschek, K.; Ribitsch, V. Cotton cellulose 1, 2, 3, 4 buthanetetracarboxylic Acid (BTCA) crosslinking monitored by some physical—Chemical methods. *Text. Res. J.* **2009**, *79*, 780–791. [CrossRef]
4. Gorgieva, S. Bacterial cellulose as a versatile platform for research and development of biomedical materials. *Processes* **2020**, *8*, 624. [CrossRef]
5. Seabra, A.B.; Bernardes, J.S.; Fávaro, W.J.; Paula, A.J.; Durán, N. Cellulose nanocrystals as carriers in medicine and their toxicities: A review. *Carbohydr. Polym.* **2018**, *181*, 514–527. [CrossRef] [PubMed]
6. Haq, I.U.; Qaisar, K.; Nawaz, A.; Akram, F.; Mukhtar, H.; Zohu, X.; Xu, Y.; Mumtaz, M.W.; Rashid, U.; Ghani, W.A.W.A.K.; et al. Advances in valorization of lignocellulosic biomass towards energy generation. *Catalysts* **2021**, *11*, 309. [CrossRef]
7. Photphisutthiphong, Y.; Vatanyoopaisarn, S. The production of bacterial cellulose from organic low-grade rice. *Curr. Res. Nutr. Food Sci.* **2020**, *8*, 206–216. [CrossRef]
8. Vigentini, I.; Fabrizio, V.; Dellacà, F.; Rossi, S.; Azario, I.; Mondin, C.; Benaglia, M.; Foschino, R. Set-Up of Bacterial cellulose production from the genus *Komagataeibacter* and its use in a gluten-free bakery product as a case study. *Front. Microbiol.* **2019**, *10*, 1953. [CrossRef]
9. Akintunde, M.O.; Adebayo-Tayo, B.C.; Ishola, M.M.; Zamani, A.; Horváth, I.S. Bacterial cellulose production from agricultural residues by two *Komagataeibacter* sp. strains. *Bioengineered* **2022**, *13*, 10010–10025. [CrossRef]
10. Paximada, P.; Kanavou, E.; Mandala, I.G. Effect of rheological and structural properties of bacterial cellulose fibrils and whey protein biocomposites on electrosprayed food-grade particles. *Carbohydr. Polym.* **2020**, *241*, 116319. [CrossRef]
11. Betlej, I.; Rybak, K.; Nowacka, M.; Antczak, A.; Borysiak, S.; Krochmal-Marczak, B.; Lipska, K.; Boruszewski, P. Structural properties of bacterial cellulose film obtained on a substrate containing sweet potato waste. *Crystals* **2022**, *12*, 1191. [CrossRef]
12. Azmi, S.N.N.S.; Fabli, S.N.N.F.M.; Aris, F.A.F.; Samsu, Z.A.; Asnawi, A.S.F.M.; Yusof, Y.M.; Ariffin, H.; Abdullah, S.S.S. Fresh oil palm frond juice as a novel and alternative fermentation medium for bacterial cellulose production. *Mater. Today Proc.* **2021**, *42*, 101–106. [CrossRef]
13. Rodrigues da Silva, I.G.; dos Santos Pantoja, B.T.; Rodrigues Almeida, G.H.; Carreira, A.C.O.; Miglino, M.A. Bacterial cellulose and ECM hydrogels: An innovative approach for cardiovascular regenerative medicine. *Int. J. Mol. Sci.* **2022**, *23*, 3955. [CrossRef] [PubMed]
14. Ayyappan, V.G.; Vhatkar, S.S.; Bose, S.; Sampath, S.; Das, S.K.; Samanta, D.; Mandal, A.B. Incorporations of gold, silver and carbon nanomaterials to kombucha-derived bacterial cellulose: Development of antibacterial leather-like materials. *J. Indian Chem. Soc.* **2022**, *99*, 100278. [CrossRef]
15. Neděla, O.; Slepička, P.; Švorčík, V. Surface modification of polymer substrates for biomedical applications. *Materials* **2017**, *10*, 1115. [CrossRef]
16. Wu, Y.; Wang, Y.; Wang, F.; He, J.; Huang, Y. Preparation and properties study of polylactic acid/bacterial cellulose composite scafolds by solvent removal. *J. Mater. Res.* **2022**, *37*, 1602–1611. [CrossRef]
17. Lupaşcu, R.E.; Ghica, M.V.; Dinu-Pîrvu, C.-E.; Popa, L.; Velescu, B.Ş.; Arsene, A.L. An overview regarding microbial aspects of production and applications of bacterial cellulose. *Materials* **2022**, *15*, 676. [CrossRef] [PubMed]
18. Zhou, L.; Fu, J.; Bian, L.; Chang, T.; Zhang, C. Preparation of a novel curdlan/bacterial cellulose/cinnamon essential oil blending film for food packaging application. *Int. J. Biol. Macromol.* **2022**, *212*, 211–219. [CrossRef]
19. Barlak, M.; Wilkowski, J.; Boruszewski, P.; Zagórski, J.; Werner, Z. Influence of electron pulses on roughness and wettability of beech wood surface. *Ann. WULS—SGGW For. Wood Technol.* **2017**, *98*, 16–19.
20. Popok, V.N. Ion implantation of polymers: Formation of nanoparticulate materials. *Rev. Adv. Mater. Sci.* **2012**, *30*, 1–26.
21. Leveneur, J.; Rajan, A.; McDonald-Wharry, J.; Le Guen, M.-J.; Pickering, K.; Kennedy, J. Structural and chemical changes of cellulose fibres under low energy ion implantations. *Surf. Coat. Technol.* **2018**, *355*, 191–199. [CrossRef]
22. Shanthini, G.M.; Sakthivel, N.; Menon, R.; Nabhiraj, P.Y.; Gómez-Tejedor, J.A.; Meseguer-Dueñas, J.M.; Ribelles, J.L.G.; Krishna, J.B.M.; Kalkura, S.N. Surface stiffening and enhanced photoluminescence of ion implanted cellulose—polyvinyl alcohol—silica composite. *Carbohydr. Polym.* **2016**, *153*, 619–630. [CrossRef]
23. Zhang, N.; Jiang, J.; Li, X.; Tong, Y. Effect of low energy ion beam implantation on the microstructure of cellulose. *Radiat. Phys. Chem.* **2011**, *80*, 990–993. [CrossRef]

24. Betlej, I.; Barlak, M.; Wilkowski, J.; Werner, Z.; Zagórski, J.; Lipska, K.; Boruszewski, P. Wettability of the surface of bacterial cellulose film modified with the ion implantation. *Ann. WULS—SGGW For. Wood Technol.* **2022**, *118*, 15–21. [CrossRef]
25. Bilek, M.M.; McKenzie, D.R. Plasma modified surfaces for covalent immobilization of functional biomolecules in the absence of chemical linkers: Towards better biosensors and a new generation of medical implants. *Biophys. Rev.* **2010**, *2*, 55–65. [CrossRef]
26. Švorčik, V.; Prošková, K.; Hnatowicz, V.; Rybka, V. Iodine penetration and doping of ion-modified polyethylene. *Nucl. Instrum. Methods Phys. Res. Sect. B* **1999**, *149*, 312–318. [CrossRef]
27. Betlej, I.; Salerno-Kochan, R.; Jankowska, A.; Krajewski, K.; Wilkowski, J.; Rybak, K.; Nowacka, M.; Boruszewski, P. The impact of the mechanical modification of bacterial cellulose films on selected quality parameters. *Coatings* **2021**, *11*, 1275. [CrossRef]
28. Barlak, M.; Wilkowski, J.; Szymanowski, K.; Czarniak, P.; Podziewski, P.; Werner, Z.; Zagórski, J.; Staszkiewicz, B. Influence of the ion implantation of nitrogen and selected metals on the lifetime of WC-Co indexable knives during MDF machining. *Ann. WULS—SGGW For. Wood Technol.* **2019**, *108*, 45–52. [CrossRef]
29. Krivonosienko, A.W.; Nikolaev, A.G.; Li, S. Техническиеописание и инструкцияпоэксплуатациионногоисточника "Титан-3" *(Technical Descriptions and Operating Instructions of the Ion Source "Titan-3")*; Российская Академия Наук—Институт Сильноточной Электроники: Tomsk, Russia, 2001. (In Russian)
30. Brown, I.; Washburn, J. The mevva ion source for high current metal ion implantation. *Nucl. Instrum. Methods. Phys. Res. B Beam Interact. Mater. At.* **1987**, *21*, 201–204. [CrossRef]
31. Wolkenhauer, A.; Avramidis, G.; Hauswald, E.; Militz, H.; Viöl, W. Sanding vs. plasma treatment of aged wood: A comparison with respect to surface energy. *Int. J. Adhes. Adhes.* **2009**, *29*, 18–22. [CrossRef]
32. Borysiuk, P.; Krajewski, K.; Auriga, A.; Auriga, R.; Betlej, I.; Rybak, K.; Nowacka, M.; Boruszewski, P. PLA Biocomposites: Evaluation of resistance to mold. *Polymers* **2022**, *14*, 157. [CrossRef] [PubMed]
33. Chassé, M.; Ross, G.G. Effect of aging on wettability of silicon surfaces modified by Ar implantation. *J. Appl. Phys.* **2002**, *92*, 5872. [CrossRef]
34. Suzuki, Y.; Kusakabe, M.; Iwaki, M. Wettability control of polystyrene by ion implantation. *Nucl. Instrum. Methods Phys. Res. Sect. B Beam Interact. Mater. At.* **1994**, *91*, 584–587. [CrossRef]
35. Parakrajang, K.; Wanichapichart, P.; Anuntalabhochai, S.; Pitakrattananukool, S.; Yu, L.D. Ion beam modification of chitosan and cellulose membranes for simulation of Ion bombardment of plant cellenvelope. *Nucl. Instrum. Methods Phys. Res. B* **2009**, *267*, 1645–1649. [CrossRef]
36. Vasenina, I.V.; Laput, O.A.; Kurzina, I.A. Regularities of PLA mechanical property modification under ion implantation conditions. *Vacuum* **2021**, *187*, 110105. [CrossRef]
37. Kalyanasundaram, N.; Wood, M.; Freund, J.B.; Johnson, H.T. Stress evolution to steady state in ion bombardment of silicon. *Mech. Res. Commun.* **2008**, *35*, 35–56. [CrossRef]
38. Nowak, R.; Li, C.L.; Swain, M.V. Comparison of implantation with Ni^{2+} and Au^{2+} ions on the indentation response of sapphire. *Mater. Sci. Eng. A* **1998**, *253*, 167–177. [CrossRef]

Disclaimer/Publisher's Note: The statements, opinions and data contained in all publications are solely those of the individual author(s) and contributor(s) and not of MDPI and/or the editor(s). MDPI and/or the editor(s) disclaim responsibility for any injury to people or property resulting from any ideas, methods, instructions or products referred to in the content.